Influence of cutting process mechanics on surface integrity and electrochemical behavior of OFHC copper

Lamice Denguir[a],*, José Outeiro[a], Guillaume Fromentin[a],

Vincent Vignal[b,d], Rémy Besnard[c,d]

[a]*LaBoMaP, Arts et Métiers ParisTech71250 Cluny, FRANCE*
[b]*ICB UMR 6303 CNRS-Université de Bourgogne, 21078 Dijon, France*
[c]*CEA Valduc, 21120 Is sur Tille, France*
[d]*LIMPE (Interaction Matériau-Procédé-Environnement), LRC DAM-VA-11-02, France*
* Corresponding author. Tel.: +33-03-85-59-53-88; fax: +33-03-85-59-53-88.*E-mail address*: Lamice.DENGUIR@ensam.eu.

Abstract

Superfinishing machining has a particular impact on cutting mechanics, surface integrity and local electrochemical behavior. In fact, material removal during this process induces geometrical, mechanical and micro-structural modifications in the machined surface and sub-surface. However, a conventional 3D cutting process is still complex to study in terms of analytical/numerical modeling and experimental process monitoring. So, researchers are wondering if a less intricate configuration such as orthogonal cutting would be able to provide information about surface integrity as close as possible to that one generated by a 3D cutting process. For that reason, in the present paper, two different machining configurations were compared: face turning and orthogonal cutting. The work material is oxygen free high conductivity copper (OFHC) and the cutting tools are uncoated cemented carbide. The research work was performed in three steps. In the first step, the process mechanics of superfinishing machining of OFHC copper was performed. In the second step, the surface integrity and the chemical behavior of the machined samples were analyzed. Finally, in the third step, correlations between input parameters and output measures were conducted using statistical techniques. Results show that when applying low ratios between the uncut chip thickness and the cutting edge radius, the surface integrity and cutting energy are highly affected by the ploughing phenomenon. Otherwise, the most relevant cutting parameter is the feed. In order to compare face turning with orthogonal cutting, a new geometrical parameter was introduced, which has a strong effect in the electrochemical behavior of the machined surface.

Keywords: Superfinishing; Surface Integrity; Corrosion Resistance; OFHC copper.

1. Introduction

Superfinishing turning is a machining process with increasing importance in industry, especially when the improvement of the functional performance and the life of the machined component are the major requirements. This target implies the control of phenomena induced by the machining process. Indeed, several research studies try to explain and predict surface integrity modifications induced by mechanical and thermal loadings generated during the cutting process. In fact, this work aims to investigate the surface integrity changes induced by superfinishing turning of oxygen free high conductivity copper (OFHC) and its impact on corrosion resistance.

1.1. . Impact of machining on surface integrity

Surface integrity is characterized in terms of topological, mechanical and metallurgical states [1,2]. Literature has shown that, when applying low ratios between the uncut chip thickness and the cutting edge radius, often found in finishing operations, the ploughing phenomenon can compete directly with the cutting

process thus changing the thermo-mechanical loadings acting in the workpiece [2,9]. As a consequence, the surface integrity will be affected, and so the functional performance and life of the machined component as well [3].

It was shown that, a material having high dislocation density undergoes a microstuctural changes due to temperature increase and high strain rate during cutting [4]. In the case of pure copper, this fact is reflected by a noticeable grains refinement induced by the dynamic recrystallization [5]. Residual stresses have been analyzed by several researchers [8,9], and explanations are also provided based on the fundamental mechanisms for residual stress formation in machining. Some researchers put into evidence the strong influence of the mechanical phenomenon caused by the tool action on the workpiece in the residual stress formation [6], while others claim that the thermal effect is the main responsible for these stresses [7].

1.2. Corrosion resistance

Concerning the corrosion resistance of the machined surface, several studies have shown that it strongly depends on the surface integrity. Bissey-Breton et al. [10,13] found that surface roughness and surface residual stresses are highly correlated with the free corrosion potential, when compared to other surface integrity parameters and machining conditions. Robin et al. [11] found that the corrosion resistance of copper decreases with the strain intensity induced by the swaging process. Yin et al. [12] showed also that the initial grain size, grain boundaries and twins have an impact on the in-depth residual stresses distribution which affects corrosion wear of copper surfaces when exposed to NaCl solution.

1.3. Presentation of the study

This paper studies the influence of superfinishing turning conditions on the surface integrity and corrosion resistance of oxygen free high conductivity copper (OFHC). This study was carried out in three steps, which uses both analytical approaches and experimental techniques. The first step is to compare the complex tridimensional superfinishing face turning geometry with the simpler orthogonal cutting one. Since this paper is focused on the surface integrity and functional performance and life of the machined components (in this case the corrosion resistance), this comparison is based on the hypothesis that identical deformation process is applied to generate the machined surface in both operations. Therefore, surface integrity in orthogonal cutting will be similar to that one generated by 3D cutting. This will simplify the researchers' work, since 2D process investigation is simpler to perform and 2D numerical modeling is less complex than 3D

modeling. In the second step, the influence of the depth of cut and feed on the forces and on the surface integrity was investigated. Later, correlations between surface integrity and corrosion resistance were established.

2. Orthogonal cutting and face turning geometry

The objective is to compare a typical 3D turning geometry with an equivalent orthogonal cutting one. Fig.1 shows the uncut chip cross-section in face turning and in orthogonal cutting.
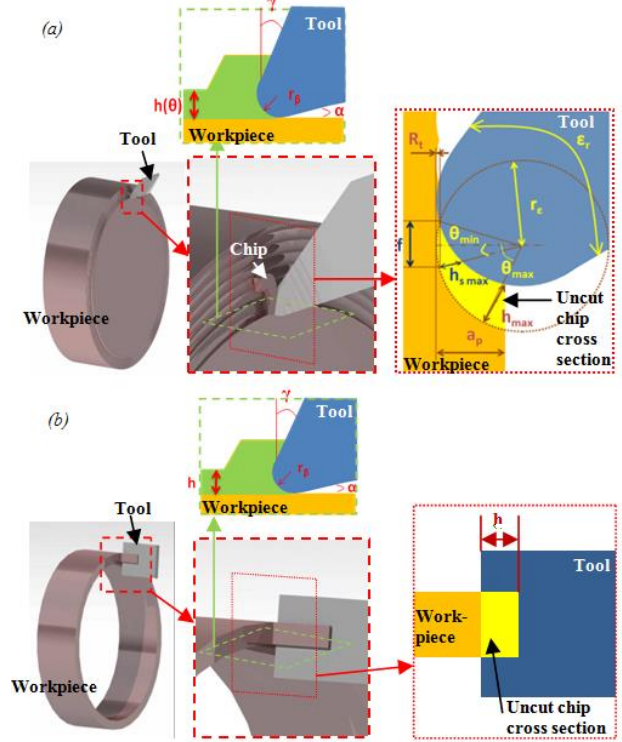

Fig. 1. Face turning (a) and orthogonal cutting (b) geometries

Based on the hypothesis that in superfinishing turning operations the depth of cut (a_p) has a minor impact on the surface integrity, an analogy can be established between the uncut chip thickness h in orthogonal cutting and the maximum local uncut chip thickness $h_{s\ max}$ in face turning. As shown in Fig. 1a, $h_{s\ max}$ is defined as the maximum local uncut chip thickness contributing to the generation of the machined surface, which can be calculated by Eq. 1.

$$_{s\ max} = r_\varepsilon + f.sin(\theta_{min}) - \sqrt{r_\varepsilon^2 - f^2.cos^2(\theta_{min})} \qquad (1)$$

where r_ε is the tool nose radius, f the feed and θ_{min} is given by Eq. 2.

$$\theta_{min} = \frac{\pi}{2} - arcos(\frac{-f}{2r_\varepsilon}) \qquad (2)$$

Therefore, machining tests were carried out using the

uncut chip thickness values shown in Table 1.

Table 1. Values of the uncut chip thicknesses *h* and $h_{s\,max}$

Orth. cutting	h [mm]	0.010	0.030	0.050
3D cutting	$h_{s\,max}$ [mm]	0.012	0.028	0.050

3. Experimental procedure and parameters

Both orthogonal cutting and face turning tests were conducted in a SOMAB T400 CNC lathe machine equipped with a piezoelectric dynamometer, used to measure the three orthogonal components of the resultant force. For both machining operations the cutting speed was kept constant and equal to 120 m/min, as well as the coolant conditions, which in this case was a compressed air cooled by a vortex system with an average temperature of -5±1°C. In orthogonal cutting, the width of cut (*b*) was kept constant and equal to 4 mm, while in face turning the depth of cut (a_p) was varied from 0.15 and 0.5 mm. The selected feed (*f*) values were 0.1, 0.15 and 0.2 mm/rev. Tungsten carbide cutting tools were used in both machining operations. The tool geometry used in face turning was the following: tool nose radius (r_ε) of 0.8 mm, tool cutting edge radius (r_n) of 9 μm, tool cutting edge angle (κ_r) of 107.5°, tool cutting edge inclination angle (λ_s) of 0°, tool normal rake angle (γ_n) of 20°, and a tool normal flank angle (α_n) of 7°. In the case of the orthogonal cutting, the tool geometry was the following: tool cutting edge radius (r_n) of 12 μm, tool normal rake angle (γ_n) of 20° and tool normal flank angle (α_n) of 5°. A total number of 9 face turning and 3 orthogonal cutting tests were performed.

The cutting forces were measured by a piezoelectric dynamometer KISTLER 9121 in the cutting (F_c), feed (F_f) and passive (F_p) directions.

The surface integrity of the machined surfaces was evaluated in terms of surface roughness and residual stresses. The surface roughness was evaluated by white light Vertical Scanning Interferometry (VSI) technique with vertical scanning resolution of 2 nm. For the samples generated by face turning, both maximum height of the profile R_t and the arithmetic average roughness R_a were evaluated in the direction normal to the feed motion, while the arithmetic mean height S_a, R_{a_peak} and R_{a_valley} parameters were evaluated in the direction parallel to the feed motion with a trace length of 2 mm. The last two parameters are the arithmetic surface roughness measured at the peak and valley of the crests (Fig. 2). For the samples generated by orthogonal cutting tests using the quick-stop device, only the parameter R_a was evaluated in the direction parallel to the cutting edge. Each surface roughness value was calculated from three measurements.
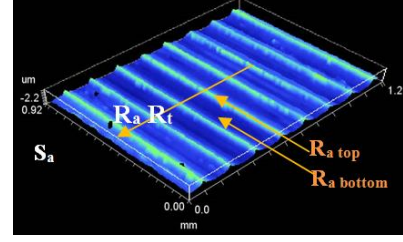

Fig. 2. Directions of roughness measurement (in 3D cutting)

As far as the residual stresses are concerned, they were analyzed by X-ray diffraction technique and applying the $\sin^2\psi$ method. According to this method, the residual stresses were calculated from strain distribution $\varepsilon_{\phi\psi\{hkl\}}$ derived from the "measured" inter reticular plane spacing and knowing the elastic radio crystallographic constants, $S_{1\{hkl\}}$ and $\frac{1}{2}S_{2\{hkl\}}$, which in this case were equal to -3.12 x 10^{-6}MPa^{-1} and 11.79 x 10^{-6}MPa, respectively. An X-ray Mn-Kα radiation was used to determine the elastic strains in the (311) planes (149° Bragg angle). Residual stresses were determined in the machined surface and subsurface, in the radial and circumferential (along the cutting direction) directions. To determine the in-depth residual stress profiles, successive layers of material were removed by electro polishing, to avoid the reintroduction of residual stress.

Concerning to the electrochemical behavior analysis, the microcell technique was used for monitoring the behavior of OFHC copper samples. Each sample was exposed to a solution of 1M $NaClO_4$ injected by a micro capillary having a diameter of 300 μm. Potentials are measured by an acquisition system in comparison with the Saturated Silver Electrode (Ag/AgCl) in room temperature (20±3°C).

Finally, correlations between different parameters were calculated using the Pearson correlation matrix method. Pearson's correlation coefficient between two series of results X and Y is calculated as shown in eq.3:

$$Correl(X,Y) = \frac{\sum(x - \bar{x})(y - \bar{y})}{\sqrt{\sum(x - \bar{x})^2 \sum(y - \bar{y})^2}} \tag{3}$$

4. Results and discussion

4.1. Cutting mechanics

This paper is focused in the generation of the machined surface, so the local forces applied to the portion of the uncut chip cross-section located between $-\theta_{min}$ and $+\theta_{min}$ is of prime concern in the case of face turning (Fig. 3).

To determine the local forces acting in this portion of the uncut chip cross-section, a force modeling method using edge discretization was applied [13]. First the total length of the cutting edges engaged was divided into 150 equal segments. Then, the three orthogonal components

of the resultant force, which were measured by the dynamometer, were distributed over the 150 segments of the cutting edge to obtain the local forces acting in each segment. These forces are then projected into cut, feed, and penetration directions.
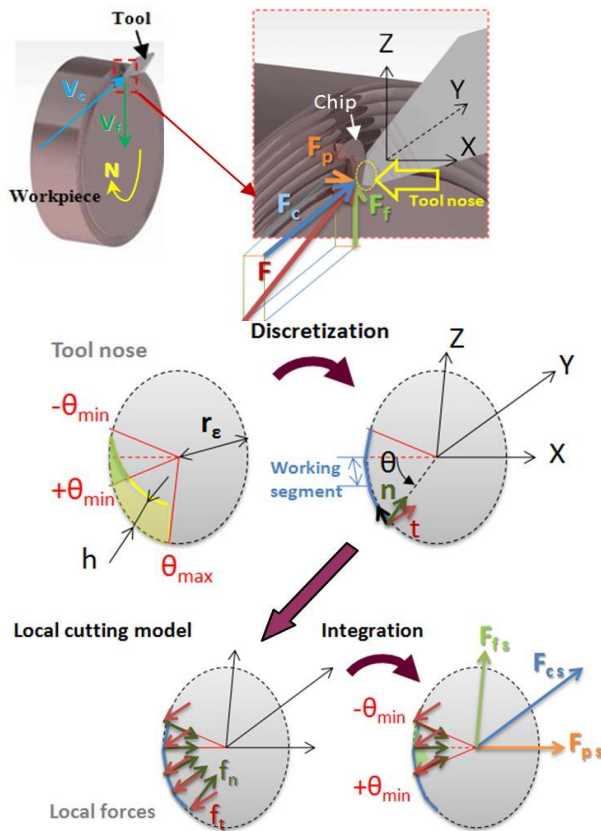

Fig. 3. Modeling local forces in face turning

Finally, the local forces acting in the portion of the uncut chip cross-section located between $-\theta_{min}$ and $+\theta_{min}$ were obtained by summing the projected forces acting in the all the segments comprised between $-\theta_{min}$ and $+\theta_{min}$ (Fig. 3).
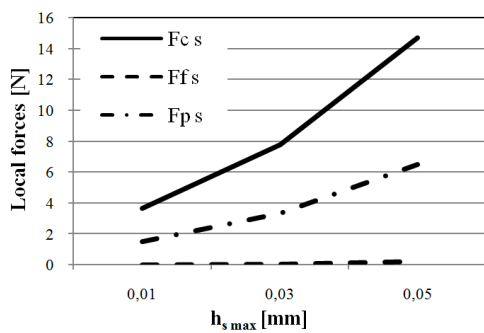

Fig. 4. Local forces in face turning in function of $h_{s\,max}$ (a_p = 0,15 mm)

Fig.4 shows a high correlation between $h_{s\,max}$ and local forces (F_{cs} - cutting force; F_{fs} - feed force; F_{ps} -

passive force acting in the previous mentioned uncut chip cross-section). Identical results were obtained for the other values of a_p, which suggest that the local forces are independent of the depth of cut a_p.

4.2. Surface integrity

a) Surface roughness

For face turning, the results have shown that although R_{a_peak} and R_{a_valley} aren't affected by the tool geometry, they are affected by $h_{s\,max}$. Indeed, $h_{s\,max}$ is correlated to R_a, R_t and S_a by more than 97% (Fig. 5). As far as orthogonal cutting is concerned, the influence of the uncut chip thickness on the surface roughness is opposite (Fig. 5). This evolution can be explained by the tool vibration, which can be caused by the ploughing phenomenon, usually observed when h is on the same magnitude or lower than the cutting edge radius r_n. In addition, for $h>0.05$ mm the surface roughness reaches a steady state, and eventually only depends of the tool wear.
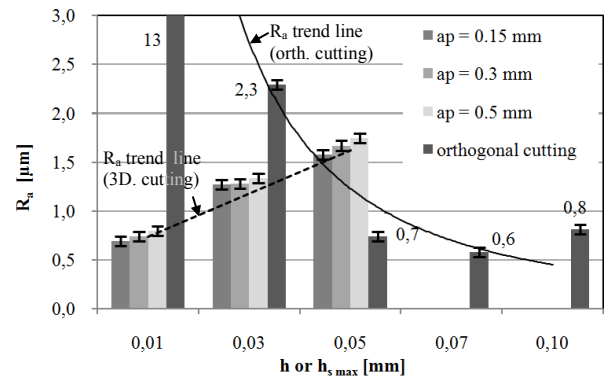

Fig. 5. Arithmetic surface roughness R_a in face turning in function of $h_{s\,max}$ and a_p and in orthogonal cutting

b) Residual stresses

The residual stresses at the machined surface were determined in the circumferential (Fig. 6) and radial (Fig. 7) directions. Only the samples machined in face turning with a_p = 0.3 mm and all the samples machined in orthogonal cutting were analyzed.
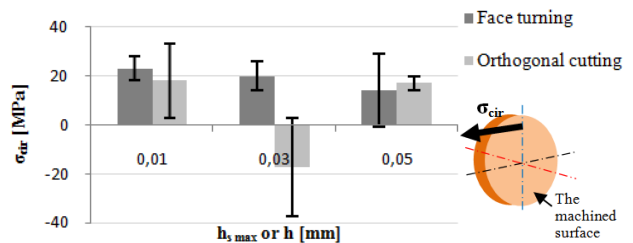

Fig. 6. Circumferential residual stress at samples surfaces in face turning and orthogonal cutting for different values of $h_{s\,max}$ or h
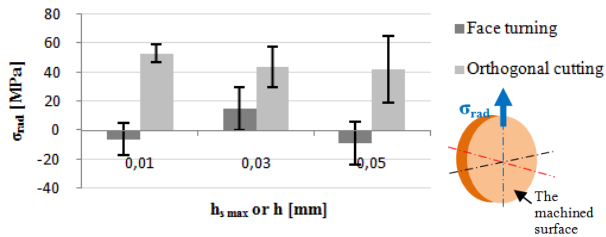
Fig. 7. Radial residual stress at samples' surface in face turning and orthogonal cutting for different values of $h_{s\,max}$ or h

Residual stresses results put into evidence the following points:

- No significant influence of either $h_{s\,max}$ (face turning) or h (orthogonal cutting) on the surface residual stresses is observed.
- In general, the surface residual stresses are tensile for both face turning and orthogonal cutting.
- Surface radial residual stress in orthogonal cutting is tensile and higher than that obtained in face turning, which is almost zero.
- Basing on Pearson correlation analysis described in §3, local forces are found inversely correlated with circumferential surface residual stresses in the case of face turning (>99%), as well as with the surface radial residual stresses in orthogonal cutting (>74%).
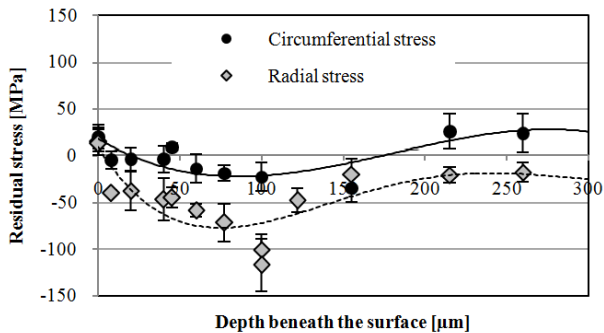

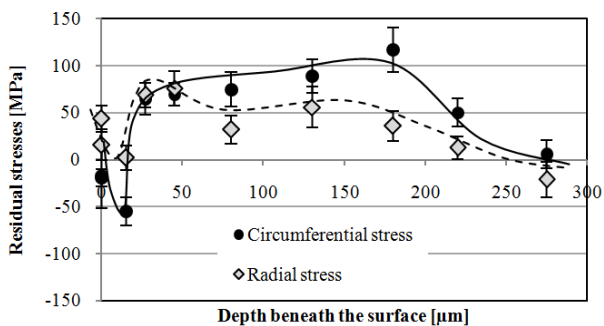Fig. 8. In depth residual stresses profiles induced by face turning ($h_{s\,max}$ = 0.03 mm)

Fig. 9. In depth residual stresses profiles induced by orthogonal cutting (h = 0.03 mm)

- Considering the distribution of the residual stresses below the machined surface measured by the

method described in [16], Fig. 8 and Fig 9 show that compressive stresses are generated by face turning, while orthogonal cutting generates tensile stresses.

4.3. Local electrochemical behavior

In this section, local electrochemical behavior of the surfaces machined by face turning and orthogonal cutting is discussed.
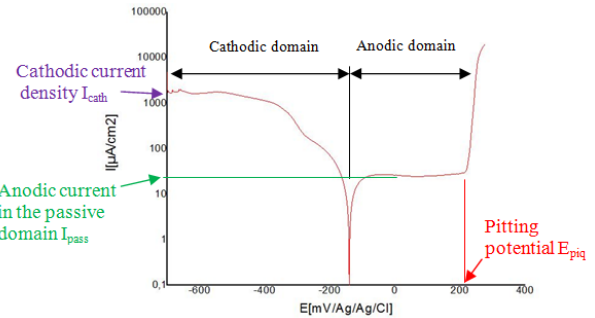

Fig. 10. Polarization curve composition

As the cathodic domain is not affected by machining in the case of OFHC copper [10] and keeps its same curve shape in all the analyzed surfaces, only anodic domain parameters show significant changes: pitting potential E_{piq} and the anodic current in the passive domain I_{pass} (fig.10). Corrosion potential E_{cor} was also measured under free corrosion conditions.
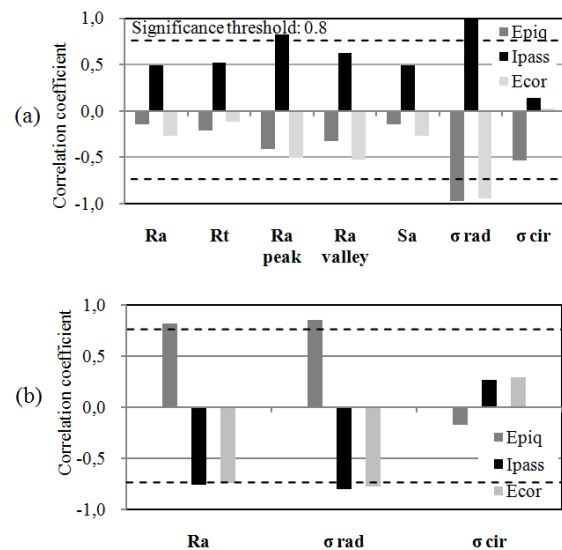

Fig. 11. Correlations between surface integrity parameters and electrochemical behavior parameters in the case of (a) face turning (b) orthogonal cutting

Surface radial stress appears as the most relevant parameter (correlation coefficient > 90%), then comes the arithmetic roughness R_a in orthogonal cutting samples (fig.11.b) and roughness parallel to feed direction characterizing the top of drag lines $R_{a\,top}$ for 3D cutting ones (fig.11.a).

Correlation results show that the anodic current in the passive domain I_{pass} is sensitive to surface topography and radial residual stress, but pitting potential and corrosion potential present more sensitivity to σ_{rad} rather than any other parameter. Indeed, the anodic current in the passive domain of copper increases with increasing residual stress [14], and the roughness influence on electronic behavior of copper was proven in previous investigations [15].
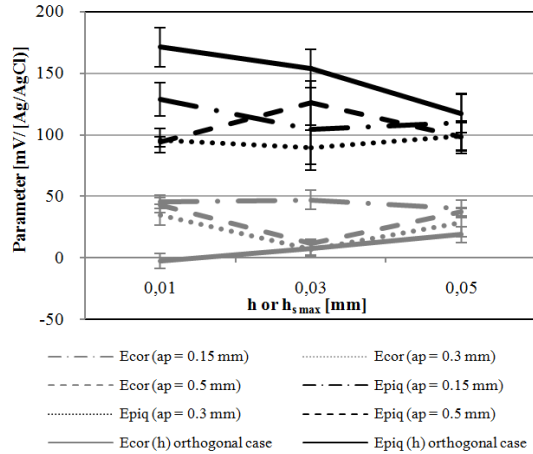

Fig. 12. E_{cor} and E_{piq} evolution considering the thickness of cut

Comparing h and $h_{s\ max}$ influence on the electrochemical parameters, it is found that the higher the uncut chip thickness is, the more the behavior of surfaces generated by orthogonal cutting and surfaces generated by face turning electrochemical converge to a comparable state (fig.12). However, in view of the dispersion found in the measured values (~50 mV), it appears likely that those findings can't yet be taken for granted, and perhaps further investigations are needed.

5. Conclusion and outlook

This work shows the impact of the superfinishing machining in the cutting mechanics, surface integrity and local electrochemical behavior. Two operations were investigated: 3D face turning and orthogonal cutting. The results have shown that the uncut chip thicknesses $h_{s\ max}$ (face turning) and h (orthogonal cutting) are strongly correlated to the local forces and surface roughness, but not to the surface residual stresses. Concerning to the in-depth residual stress profiles, face turning generates a thicker layer of compressive residual stresses, while orthogonal cutting generates a thicker layer of tensile residual stresses. Finally, correlation analysis between local electrochemical behavior and surface integrity parameters has proven that R_{a_peak} (face turning) and R_a (orthogonal cutting) are the most influencing parameters on the local electrochemical behavior.

The present results are not enough to confirm the hypothesis that identical deformation process is applied to generate the machined surface in both superfinishing turning and orthogonal cutting. Thus, further experiments are required with a closer analysis to the thermal and mechanical phenomena developed at the tool flank contact. These phenomena will be investigated experimentally and numerically.

References

[1] Field M., Kahles J.F., 1964. "The Surface Integrity of Machined and Ground High Strength Steels," DMIC Report 210, p.54–77.
[2] Albrecht P., 1960. "New development in the theory of the metal cutting process, part I: The ploughing process in metal cutting," J. of Engineering and Industry, ASME, 348.
[3] Jawahir I. S. Brinksmeier E. M'Saoubi R. Aspinwall D. K. Outeiro J. C. Meyer D. Umbrella D. Jayal A. D., 2011, "Surface integrity in material removal processes: recent advances, Manufacturing Technology 60," CIRP Annals, p. 603-626.
[4] Ni.H, Alpas A. T., 2003. "Sub-micrometer structures generated during dry machining of copper," Material Science and Engineering A365, p. 338-349.
[5] Gravier J., 2009. Impact de l'usinage en superfinition sur la zone affectée par le procédé, Thèse de doctorat mention Sciences, spécialité physique chimie, ICB.
[6] Henriksen E.K., 1951. "Residual stresses in machined surfaces," Trans. ASME, p. 69-76.
[7] Liu C. R., Barash M.M., 1976. "The mechanical state of the sublayer of a surface generated by chip-removal process—part I cutting with a sharp tool," Trans. ASME, J. Eng. Ind, p. 1192–1201.
[8] Capello E., 2004, "Residual stresses in turning, Part I: Influence of process parameters," Journal of Materials Processing Technology 160; p. 221-228.
[9] Outeiro, J.C., 2007. "Influence of tool sharpness on the thermal and mechanical phenomena generated during machining operations," Int. J. Machining and Machinability of Materials 2, p. 413–432.
[10] Bissey-Breton S., Gravier J., Vignal V., 2011. "Impact of superfinish turning on surface integrity of pure copper," 1st CIRP conference on surface integrity (CSI), Procedia Engineering 19, p. 28-33.
[11] Robin A., Martinez G., Suzuki P., 2012. "Effect of cold working process on corrosion behavior of copper," Materials and Design, 34, p. 319-324.
[12] Yin S., Li D. Y., 2005. "Effects of prior cold working on corrosion and corrosive wear of copper in HNO and NaCl solutions," Materials Science and Engineering A394, p. 266-276.
[13] Armarego E.J.A., Whitfield R.C., 1985, "Computer based modelling of popular machining operations for force and power prediction," CIRP Annals - Manufacturing Technology 34, p. 65-69.
[14] Gravier J., Vignal V., Bissey-Breton S., 2008. "The use of linear regression methods and Pearson's correlation matrix to identify mechanical-physical-chemical parameters controlling the micro-electrochemical behavior of machined copper," Corrosion Science 50, p. 2885-2894.
[15] Gravier J., Vignal V., Bissey-Breton S., 2012. "Influence of residual stress, surface roughness and crystallographic texture induced by machining on the corrosion behavior of copper in salt-fog atmosphere," Corrosion Science 61, p. 162-170.
[16] I.C. Noyan, J.B. Cohen, 1987, "Residual Stress—Measurement by Diffraction and Interpretation", Springer, New York.